# THERMO-FLUID-STRUCTURAL ANALYSIS OF A GLOBE VALVE

Bruno Seixas
*Independent Researcher / Mechanical Engineer*

**ABSTRACT**
This work presents a multiphysics thermo-fluid-structural analysis of a globe valve, aiming to evaluate the behavior of its components subjected to thermal and pressure loading under different flow conditions. Initially, a fluid dynamics (CFD) analysis was performed in Fluent to obtain the velocity and pressure fields of the flow. Subsequently, a steady-state thermal analysis was performed to obtain the temperature fields. The pressure and temperature fields obtained were used as boundary conditions for a structural analysis. This work allowed us to obtain the stresses and displacements in the valve components and establish a correlation between the operating conditions and the structural behavior of the valve.

**Keywords** : Globe valve. Thermo-fluid-structural analysis. Ansys Mechanical. Ansys Fluent.

## 1. INTRODUCTION

Globe valves are mechanical devices used for flow control and blocking in piping systems, especially in applications requiring precise flow regulation. Globe valves are widely used in steam, water, oil, and gas systems, in chemical, petrochemical, and power generation industries, as well as in industrial and laboratory process installations. They are preferred in situations where finer flow control is needed. Some applications of globe valves include: steam control in boilers and turbines, cooling and heating lines, pressure and flow control systems in chemical plants, precision hydraulic and pneumatic circuits, and process lines in refineries and power plants.

A globe valve is composed of several mechanical elements that, together, allow for the blocking and control of fluid. The main parts and their functions are:

- Body: This is the main casing of the valve, responsible *for* withstanding internal pressure and directing fluid flow.
- Bonnet: component that closes the upper part of the body and houses the shaft (rod) sealing system. It also serves as a support structure for the actuator or handwheel.
- Plug or *Disc: a* movable element that blocks or regulates the flow. Its vertical movement brings the plug closer to or further away from the seat, controlling the passage of the fluid.
- Seat: fixed surface against which the shutter rests to create a seal.

- Stem: transmits the movement of the actuator (manual or automatic) to the shutter. It is usually threaded and guided by gaskets to prevent leaks.
- Packings: sealing rings *arranged* around the stem, preventing fluid leakage into the environment.
- Actuator or Handwheel*:* a device that operates the valve, which can be manual (handwheel), electric, pneumatic, or hydraulic, depending on the application.

Figure 1 illustrates the parts of a globe valve.

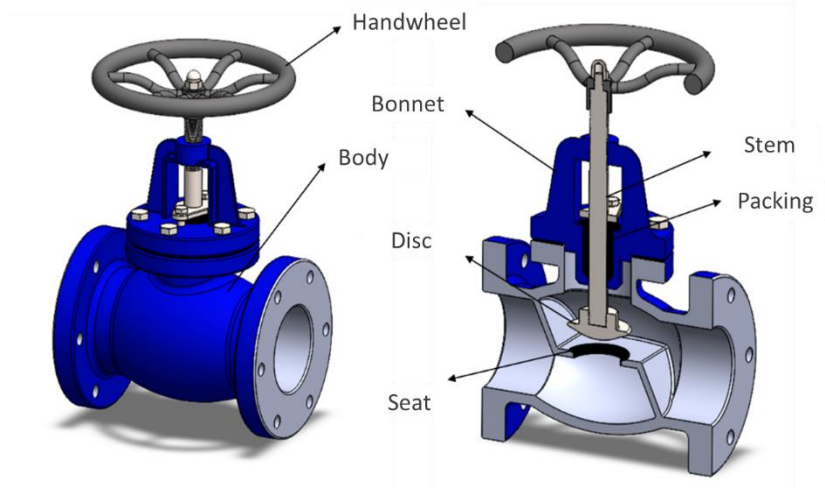


**Figure 1 –** Globe Valve.

**Source:** Author, 2025

## 2. OBJECTIVE

The objective of this work is to perform a thermo-fluid-structural evaluation of a globe valve and its components under varying operating conditions. Water flow at 60°C with an inlet velocity of 5 m/s and an outlet pressure under three conditions will be considered: 10, 15, and 20 bar.

For the present study, the valve geometry was simplified, modeling only the valve body, bonnet, stem, and obturator. Since the valve is inserted in a section of piping that impacts the flow reaching the valve, as well as the constraints imposed on the flanges, these sections of piping at the inlet and outlet were also modeled. The internal diameter of the pipes is 88.9 mm. Despite this representation of the pipes, the focus of the analysis was the structural behavior of the valve components. Furthermore, symmetry was observed throughout the problem, representing gains in computational time without compromising the quality of the results. Figure 2 illustrates the geometry considered for the problem.

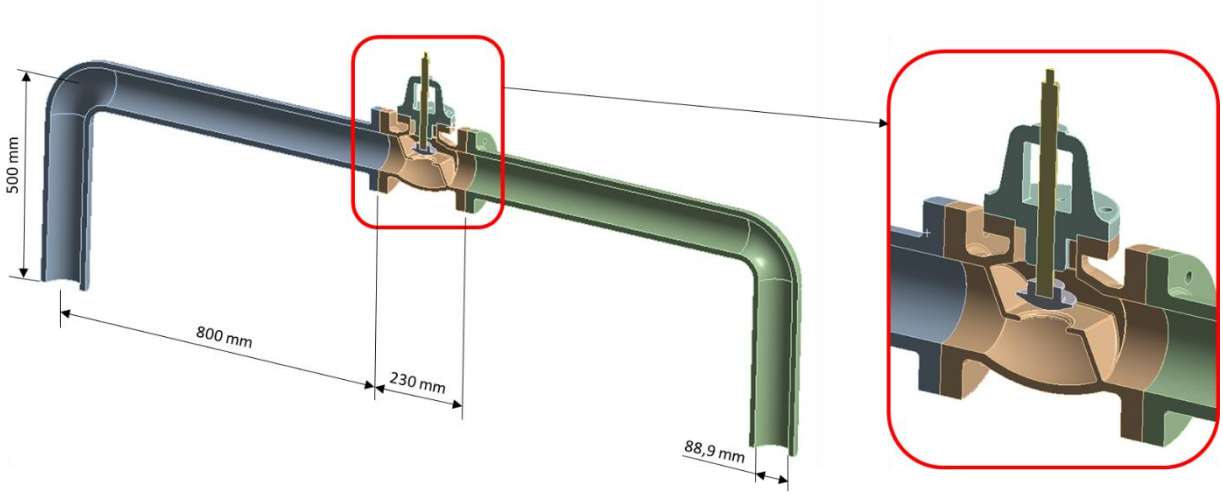


**Figure 2 –** Globe valve geometry.

**Source:** Author, 2025

The ASME B16.34 standard – *Valves – Flanged, Threaded, and Welding End* – establishes the design requirements, materials, dimensions, tests, and pressure and temperature limits for industrial valves with flanged, threaded, or welded connections. It is widely used as an international reference for the sizing and classification of process valves, ensuring safety and standardization in pressurized piping systems. In this work, the operating conditions of the globe valve are in accordance with Class 300 (*Standard Class*) for Group 1.1 of materials, as defined in ASME B16.34. According to this standard, for a temperature of 60 °C, the maximum allowable pressure is approximately 49.4 bar. Figure 3 shows the section of the standard referring to pressure and temperature classes.

**Table 2-1.1 Ratings for Group 1.1 Materials**

| | | | |
|---|---|---|---|
| A 105 (1)(2) | A 515 Gr.70 (1) | A 696 Gr. C | A 672 Gr. B70 (1) |
| A 216 GR. WCB (1) | A 516 Gr. 70 (1)(3) | A 350 Gr. LF6 Cl. 1 (4) | A 672 Gr. C70 (1) |
| A 350 Gr. LF2 (1) | A 537 Cl. 1 (5) | A 350 Gr. LF3 (6) | |

NOTES:
(1) Upon prolonged exposure to temperatures above 425C°, the carbide phase of steel may be converted to graphite. Permissible, but not recommended for prolonged usage above 425°C.
(2) Only killed steel shall be used above 455°C.
(3) Not to be used over 455°C.
(4) Not to be used over 260°C.
(5) Not to be used over 370°C.
(6) Not to be used over 345°C.

**A – Standard Class**

| Temperature, °C | Working Pressures by Class, bar | | | | | | |
|---|---|---|---|---|---|---|---|
| | 150 | 300 | 600 | 900 | 1500 | 2500 | 4500 |
| –29 to 38 | 19.6 | 51.1 | 102.1 | 153.2 | 255.3 | 425.5 | 765.9 |
| 50 | 19.2 | 50.1 | 100.2 | 150.4 | 250.6 | 417.7 | 751.9 |
| 100 | 17.7 | 46.6 | 93.2 | 139.8 | 233.0 | 388.3 | 699.0 |
| 150 | 15.8 | 45.1 | 90.2 | 135.2 | 225.4 | 375.6 | 676.1 |
| 200 | 13.8 | 43.8 | 87.6 | 131.4 | 219.0 | 365.0 | 657.0 |
| 250 | 12.1 | 41.9 | 83.9 | 125.8 | 209.7 | 349.5 | 629.1 |
| 300 | 10.2 | 39.8 | 79.6 | 119.5 | 199.1 | 331.8 | 597.3 |
| 325 | 9.3 | 38.7 | 77.4 | 116.1 | 193.6 | 322.6 | 580.7 |
| 350 | 8.4 | 37.6 | 75.1 | 112.7 | 187.8 | 313.0 | 563.5 |
| 375 | 7.4 | 36.4 | 72.7 | 109.1 | 181.8 | 303.1 | 545.5 |
| 400 | 6.5 | 34.7 | 69.4 | 104.2 | 173.6 | 289.3 | 520.8 |
| 425 | 5.5 | 28.8 | 57.5 | 86.3 | 143.8 | 239.7 | 431.5 |
| 450 | 4.6 | 23.0 | 46.0 | 69.0 | 115.0 | 191.7 | 345.1 |
| 475 | 3.7 | 17.4 | 34.9 | 52.3 | 87.2 | 145.3 | 261.5 |
| 500 | 2.8 | 11.8 | 23.5 | 35.3 | 58.8 | 97.9 | 176.3 |
| 538 | 1.4 | 5.9 | 11.8 | 17.7 | 29.5 | 49.2 | 88.6 |

**Figure 3 –** Pressure Classes as a Function of Temperature.

**Source:** ASME B16.34 Standard

## 3. CFD CONFIGURATION

### 3.1 Flow Conditions

For this study, water will flow at an inlet velocity of 5 m/s, at a constant temperature of 60°C and outlet pressures of 10, 15, and 20 bar. Under these conditions, the density of water is approximately 984 kg/m³ and the viscosity is 0.0004665 Pa.s. Despite variations in outlet pressure, the properties of the water do not change significantly with this pressure variation. To characterize the flow regime inside the valve, it is essential to calculate the Reynolds number ( $\boldsymbol{Re}$), defined by the expression:

$$Re = \frac{\rho.V.D}{\mu} = \frac{984.5.0{,}0889}{0{,}0004665} \cong 937595$$

In the equation, $\rho$is the fluid density, $V$is the average fluid velocity, $D$is the hydraulic diameter (in this case, the internal diameter of the pipe), and $\mu$is the fluid viscosity. Because the Reynolds number is much greater than 2300, the flow inside the pipe is turbulent.

### 3.2 Geometry

The fluid domain geometry was obtained from the three-dimensional model of the globe valve, using the SpaceClaim environment of the ANSYS software. To extract the region occupied by the fluid inside the valve, the " *Volume Extract* " command was used, which allows the automatic generation of the internal flow volume based on the internal surfaces of the solid part. Figure 4 shows the resulting fluid domain geometry, used as the basis for mesh generation and boundary condition definition in the simulation stage.

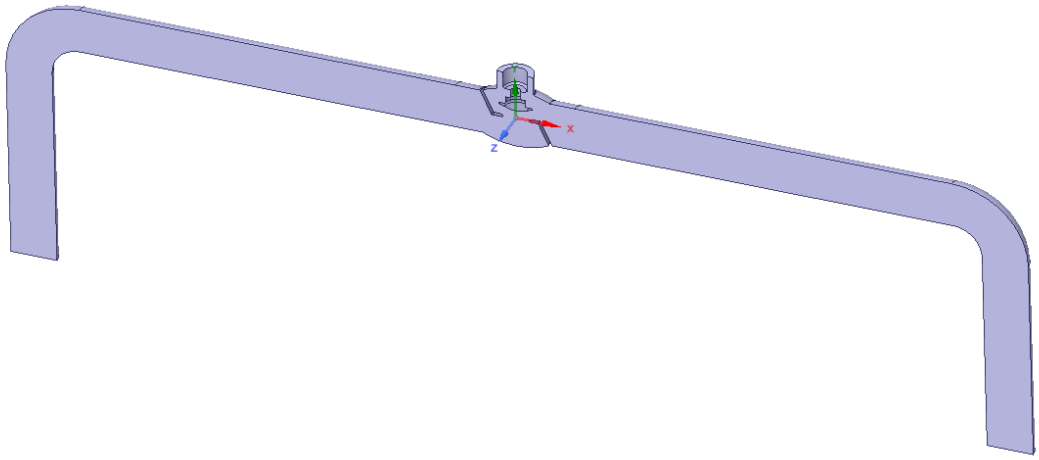

**Figure 4 –** Geometry of the fluid domain.

**Source:** Author, 2025

### 3.3 Mesh

Once the fluid domain geometry was obtained, the volume was discretized to calculate the flow. The mesh defines the points where the conservation equations (mass, momentum, and energy) will be solved numerically, and is therefore one of the most important factors in ensuring stability and accuracy in the simulation results.

In Computational Fluid Dynamics (CFD) analysis, controlling the size of the first layer of elements (the first cell next to the wall) is fundamental because this region corresponds to the boundary layer, where high velocity gradients occur. The ideal height of the first element can be estimated by the following relationship (VERSTEEG et al., 2007):

$$y = \frac{\mu}{\rho u_\tau} y^+$$

In the equation $y$, is the height of the first layer of elements next to the wall, $y^+$is the dimensionless distance from the first cell to the wall, is $\mu$the dynamic viscosity of the fluid [Pa.s], $\rho$is the density of the fluid [kg/m³], and $u_\tau$is the friction velocity [m/s]. This velocity is a function of the shear stress on the wall ( $\tau_w$), which in turn is a function of the average flow velocity ( $u_0$) and the wall friction coefficient ( $C_f$). The equations below demonstrate the calculation of all these terms and the determination of the ideal size of the first layer.

$$C_f = 0{,}079 Re^{-0{,}25} = 0{,}079.937595^{-0{,}25} \cong 0{,}0025$$

$$\tau_w = \frac{1}{2}\rho u_0^2 C_f = \frac{1}{2}.984.5^2.0{,}0025 \cong 31{,}23 \ \frac{kg}{m.s^2}$$

$$u_\tau = \sqrt{\frac{\tau_w}{\rho}} = \sqrt{\frac{31{,}23}{984}} \cong 0{,}178 \frac{m}{s}$$

$$y = \frac{\mu}{\rho u_\tau} y^+ = \frac{0{,}0004665}{984.0{,}178} 1 \cong 0{,}003\ mm$$

For the analytical calculation of the height of the first layer of elements, the value of was adopted $y^+ = 1$, since this criterion provides greater resolution of the boundary layer. The result obtained for this condition was a first cell height of approximately 0.003 mm. However, this extremely reduced thickness would require a large number of layers and elements in the

region near the wall, resulting in an excessively dense mesh and, consequently, high computational cost.

Since the main objective of this work is the evaluation of the pressure field inside the globe valve, and not the detailed analysis of the boundary layer, a first layer with a height of 0.3 mm was chosen. This choice represents a balance between precision and computational cost, ensuring that wall effects are reasonably well represented, while maintaining the numerical efficiency of the simulation. The Inflation feature was used to construct this layer. Figures 5 and 6 show the constructed mesh and the details of the Inflation layer, respectively.

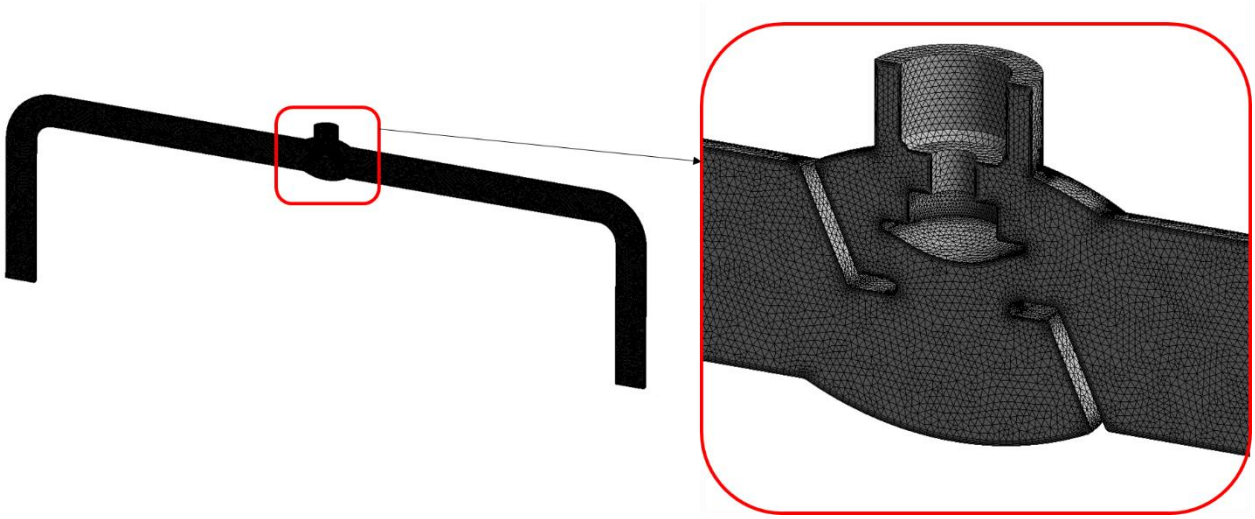

**Figure 5 –** Considered CFD mesh

**Source:** Author, 2025

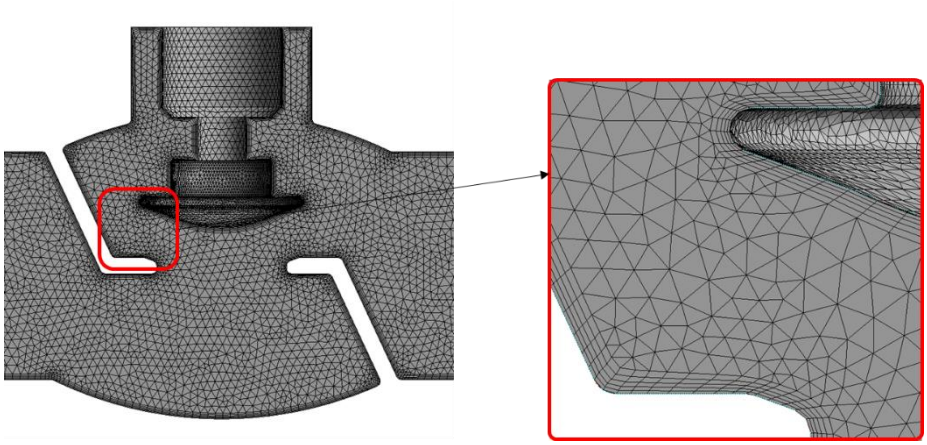

**Figure 6 –** Details of the inflation layer near the walls.

**Source:** Author, 2025

Regarding mesh quality criteria, the Skewness criterion was verified, which is highly valued in CFD analyses and measures how much the shape of an element deviates from its ideal

configuration. This parameter is important because high skewness values indicate distorted elements, which can compromise the accuracy and numerical stability of the simulation. Figure 7 shows the acceptable ranges for the Skewness criterion.

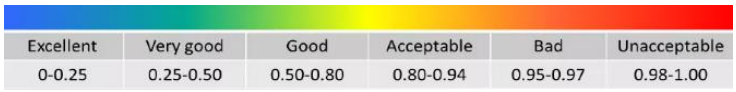

| Excellent | Very good | Good | Acceptable | Bad | Unacceptable |
|---|---|---|---|---|---|
| 0-0.25 | 0.25-0.50 | 0.50-0.80 | 0.80-0.94 | 0.95-0.97 | 0.98-1.00 |

**Figure 7 –** Skewness Criterion for Mesh Quality.

Source: ANSYS

As can be seen from Figure 8, most of the elements are within the recommended range, which ensures a suitable mesh for the proposed numerical analysis.

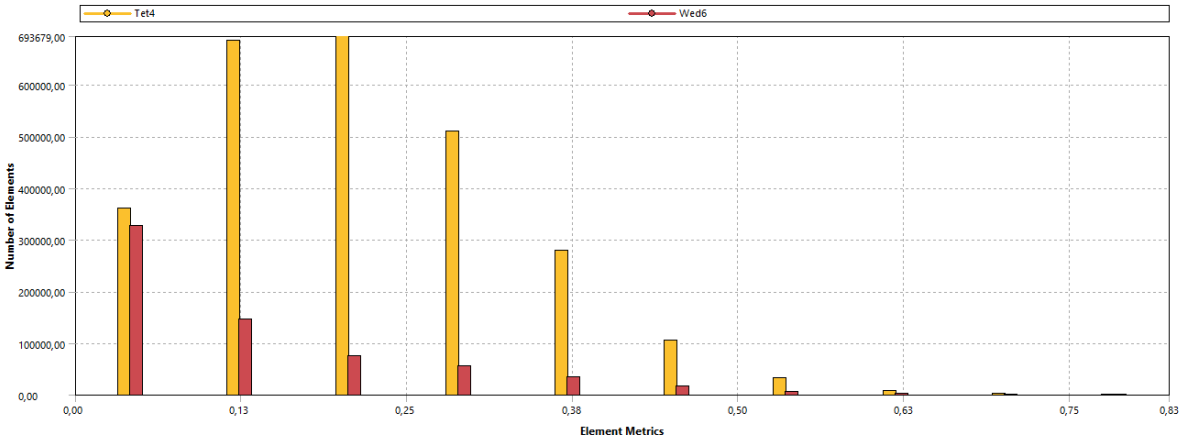


Figure 8 – Skewness Parameter of Mesh Quality.

Source: Author, 2025

### 3.3 CFD Setup

Because it is a turbulent flow, the turbulent viscosity equation was activated in ANSYS Fluent. The turbulence model adopted was k–ω SST (*Shear Stress Transport*), as it is one of the most robust and widely used models in industrial applications. This model combines the advantages of the traditional k–ω, which performs well near the walls, with those of k–ε, which performs better in regions away from the wall and in free flow.

Regarding the boundary conditions, an inlet water velocity of 5 m/s was defined *in* the inlet pipe, and outlet pressures *of* 10, 15, and 20 bar were defined, corresponding to the different cases analyzed. Furthermore, a symmetry condition was applied in ANSYS Fluent, since both the globe valve geometry and the fluid flow exhibit symmetry with respect to a longitudinal plane. This simplification allows for a reduction in the calculation domain and, consequently, the computational cost, without compromising the accuracy of the results. Figure 9 shows the boundary conditions applied in Fluent.

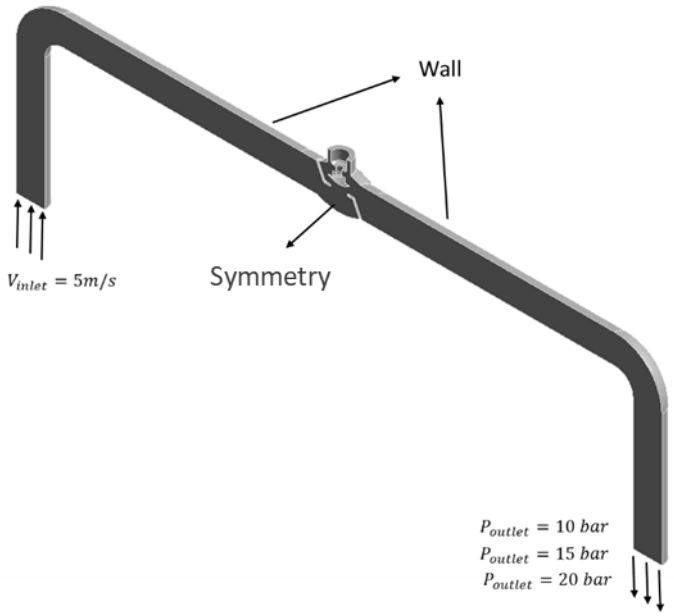


**Figure 9 –** Boundary Conditions in Fluent.

**Source:** Author, 2025

For initialization, the ANSYS Fluent hybrid model was adopted. Furthermore, a number of 200 iterations was defined for each simulated case, a value sufficient to guarantee the stabilization of the residuals and the obtaining of convergent results for the pressure and velocity fields.

### 3.4 Numerical Convergence

The inlet pressure and outlet velocity values were monitored using *Report Plots* in ANSYS Fluent, with the aim of tracking the physical convergence of the problem throughout the iterations and ensuring the stability of the results obtained. Figure 10 shows the physical convergence of the parameters.

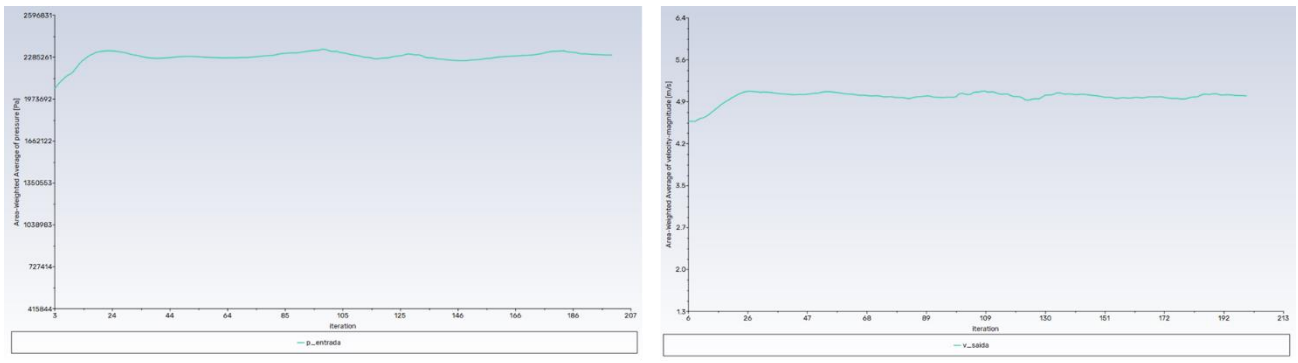


(a) (b)

**Figure 10 –** Physical Convergence of Parameters – (a) pressure and (b) velocity.

**Source:** Author, 2025

## 4. CFD RESULTS

Figures 11 to 16 show the velocity and pressure fields for each condition.

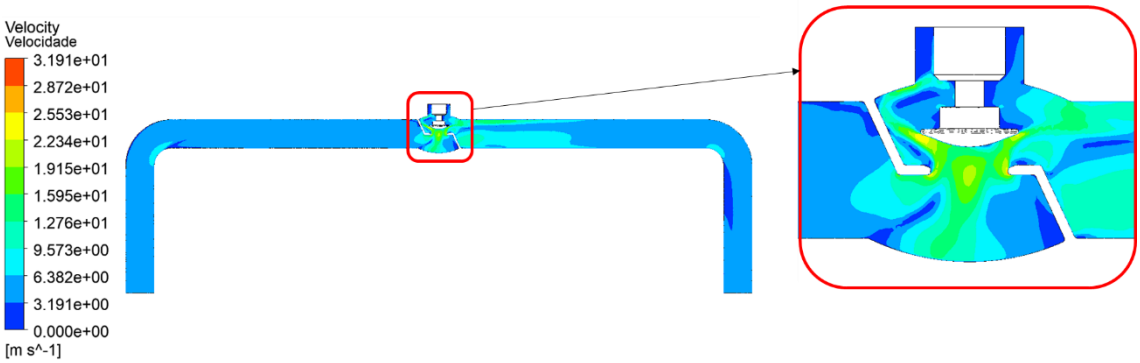


**Figure 11 –** Velocity field for an outlet pressure of 10 bar.

**Source:** Author, 2025

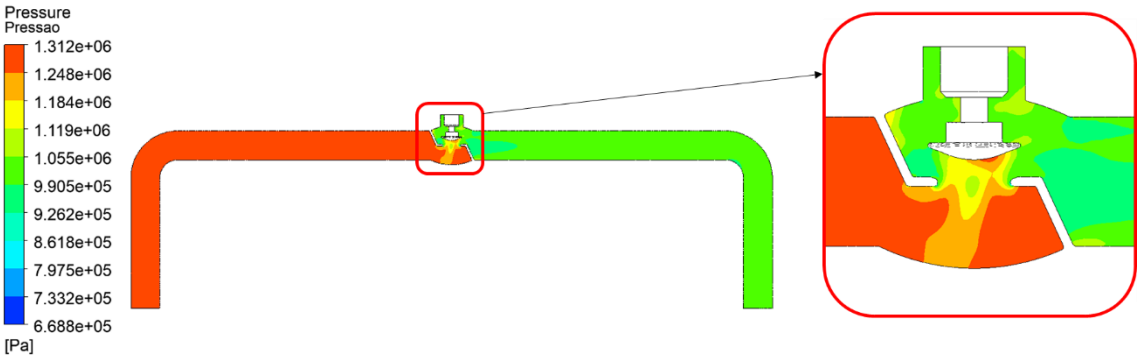


**Figure 12 –** Pressure field for an outlet pressure of 10 bar.

**Source:** Author, 2025

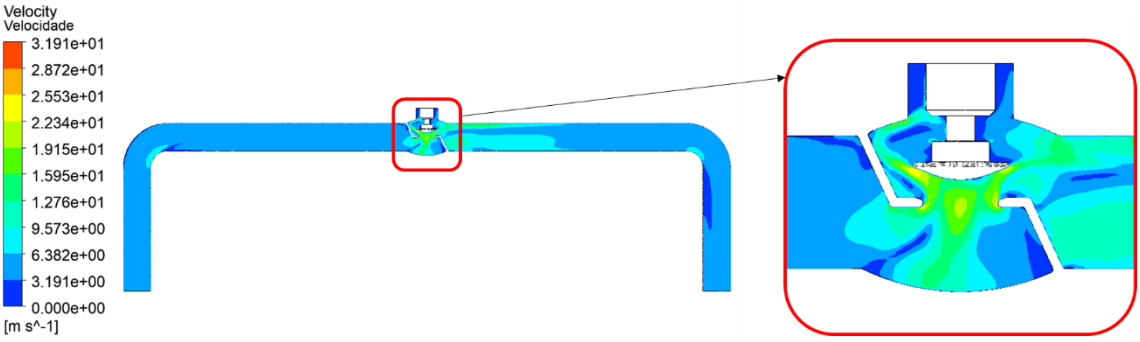


**Figure 13 –** Velocity field for an outlet pressure of 15 bar.

**Source:** Author, 2025

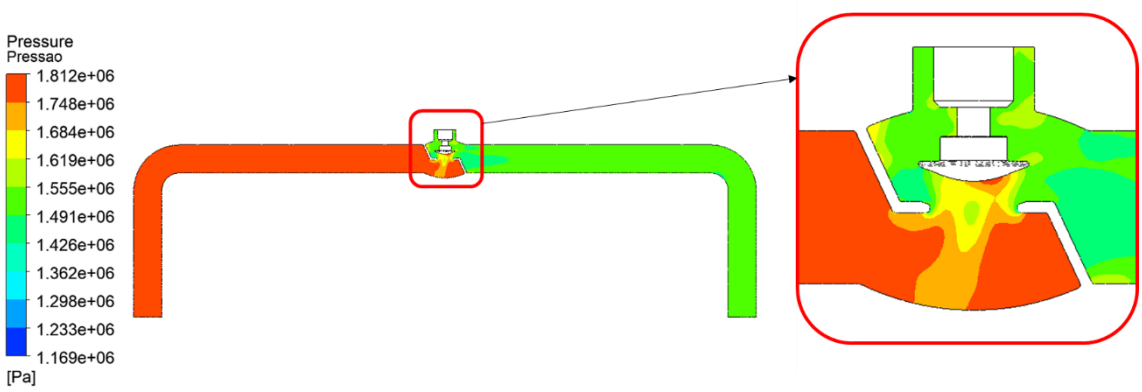


**Figure 14 –** Pressure field for an outlet pressure of 15 bar.

**Source:** Author, 2025

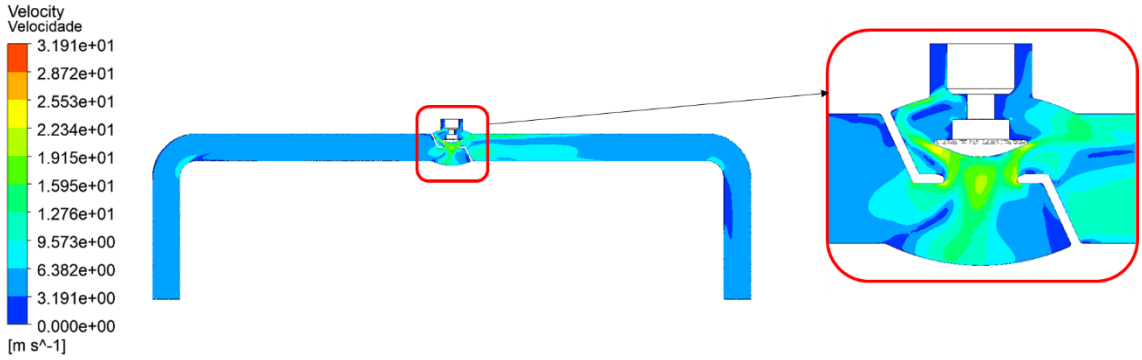


**Figure 15 –** Velocity field for an outlet pressure of 20 bar.

**Source:** Author, 2025

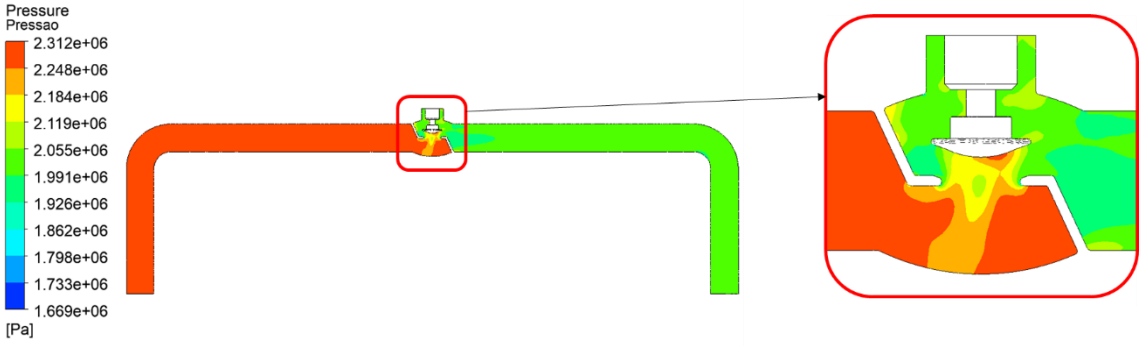


**Figure 16 –** Pressure field for an outlet pressure of 20 bar.

**Source:** Author, 2025

As can be observed, the velocity fields obtained in the different configurations exhibit similar behavior, since the velocity condition imposed at the input is the same. The pressure fields, however, while qualitatively similar, show distinct magnitudes due to the different output pressure conditions applied in each case.

## 5. STRUCTURAL CONFIGURATION

### 5.1 Fluent-Mechanical Integration

One-way FSI (*Fluid-Structure-Interaction)* integration was performed between different types of analyses in the ANSYS *Workbench environment* , with the aim of evaluating the thermo-fluid-structural behavior of the globe valve. One-way coupling was adopted because it is suitable for the case study, since the displacements of the valve components are small and do not significantly influence the flow.

Initially, a CFD analysis was performed in ANSYS Fluent to determine the pressure field resulting from the internal flow of water through the valve. Then, a steady *-state thermal analysis was performed* to obtain the temperature field in the valve body, considering the heat transfer between the fluid taken at a constant temperature, the metal walls, and the environment.

Finally, based on the pressure and temperature results obtained, a static structural analysis was conducted to evaluate the mechanical behavior of the valve components, determining the stresses, deformations, and critical regions under the established operating conditions. This import is done by connecting the *Solution* from the Fluent and Thermal Analysis to the *Setup* of the structural analysis, as illustrated in Figure 17.

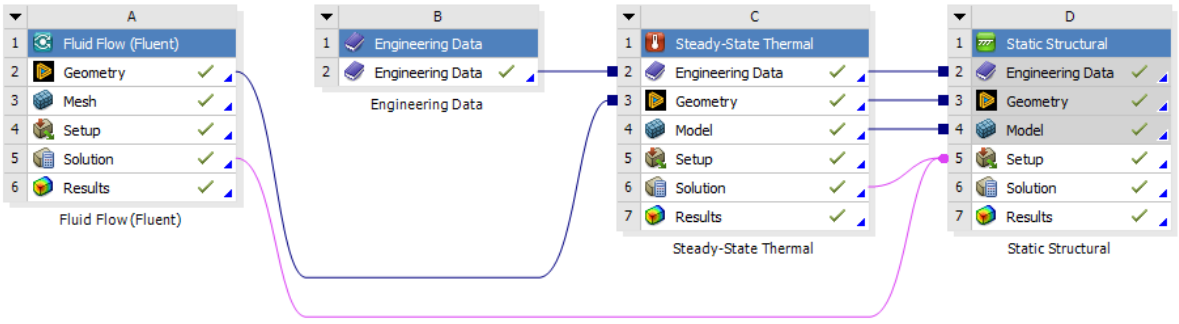


**Figure 17 –** Fluid-Thermal-Structural Coupling

**Source:** Author, 2025

### 5.2 Materials

Regarding the materials used for the analysis, ASTM A216 WCB steel was assigned to the valve body and bonnet. AISI 410 steel was used for the stem and obturator, and structural steel for the tubes. As a thermal evaluation was also performed in this work, in addition to the mechanical properties, the thermal properties of the materials were also determined, as shown in Table 1.

| | Material | Elasticity Modulus [GPa] | Poisson's Ratio [-] | Yield Strength [MPa] | Ultimate Tensile Strength [MPa] | Thermal Conductivity [W/m·K] | Coefficient of Thermal Expansion [1/°C] |
|---|---|---|---|---|---|---|---|
| Body | ASTM A216 WCB | 207 | 0,29 | 250 | 485 | 48 | 0,000012 |
| Bonnet | ASTM A216 WCB | 207 | 0,29 | 250 | 485 | 48 | 0,000012 |
| Stem | AISI 410 | 200 | 0,29 | 275 | 480 | 24,9 | 0,0000099 |
| Disc | AISI 410 | 200 | 0,29 | 275 | 480 | 24,9 | 0,0000099 |
| Tubes | Structural Steel | 200 | 0,3 | 250 | 460 | 60,5 | 0,000012 |

**Table 1 –** Mechanical and Thermal Properties of Materials

**Source:** Author, 2025

### 5.3 Thermal Analysis

The thermal analysis aims to obtain the temperature field in the structure to be imported into the static structural model. In the thermal analysis, a fixed temperature of 60°C was considered for the fluid flowing through the piping and valve. Furthermore, heat exchange via convection and radiation was considered on the external surfaces of the geometry with the environment.

To determine an estimated convection coefficient ( $h$), a transverse airflow around a cylinder (tube geometry) at a velocity of 5 m/s was considered. The coefficient can be estimated from the calculation of the Nusselt number ( $Nu$), according to the equation below (INCROPERA et al., 2011).

$$Nu = C.Re^{m}.Pr^{1/3}$$

In the equation, $Re$is the Reynolds number, $Pr$is the Prandtl number, and $C$and $m$are constants that depend on the flow conditions. Considering the following properties of air: density (ρ $\rho$) = 1.18 kg/m³, viscosity (μ $\mu$) = 0.0000185 Pa.s, conductivity (μ $k$) = 0.0262 W/mK, and specific heat (μ $c_p$) = 1007 J/kg, and considering the outer diameter of the tube to be 118.9 mm (15 mm wall thickness), we can calculate $Re$and $Pr$as follows:

$$Re = \frac{\rho.V.D}{\mu} = \frac{1{,}18.5.0{,}1189}{0{,}0000185} \cong 37919$$

$$Pr = \frac{c_{P}.\mu}{k} = \frac{1007.0{,}0000185}{0{,}0262} \cong 0{,}711$$

Since the Reynolds number is between 4000 and 40,000, the values of the coefficients $C$are $m$0.193 and 0.618, respectively. Therefore, the Nusselt value and then the coefficient h can be calculated as follows:

$$Nu = C.Re^{m}.Pr^{1/3} = 0{,}193.(37919^{0{,}193}).(0{,}711^{0{,}618}) = 116{,}39$$

$$h = \frac{Nu.k}{D} = \frac{116{,}39.0{,}0262}{0{,}1189} = 25{,}6\frac{W}{m^2.K}$$

Although this value was calculated for a cylinder, which is a good approximation for the tube regions, the same value was adopted for the outer surfaces of the valves in an approximate manner.

Regarding radiation exchange with the environment, an emissivity of 0.79 was considered across the entire outer surface (equivalent to oxidized carbon steel). An ambient temperature of 22°C was considered for both convection and radiation. Figure 18 illustrates the boundary conditions considered for thermal analysis.


**Figure 18 –** Thermal Boundary Conditions

**Source:** Author, 2025

Next, the thermal analysis was run and the temperature field in the model was obtained, as illustrated in Figures 19 and 20.

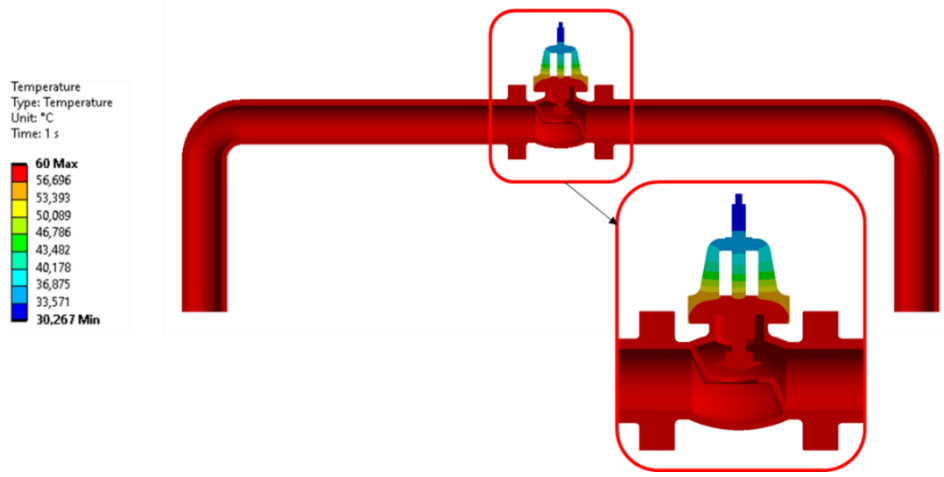


**Figure 19 –** Temperature Field

**Source:** Author, 2025

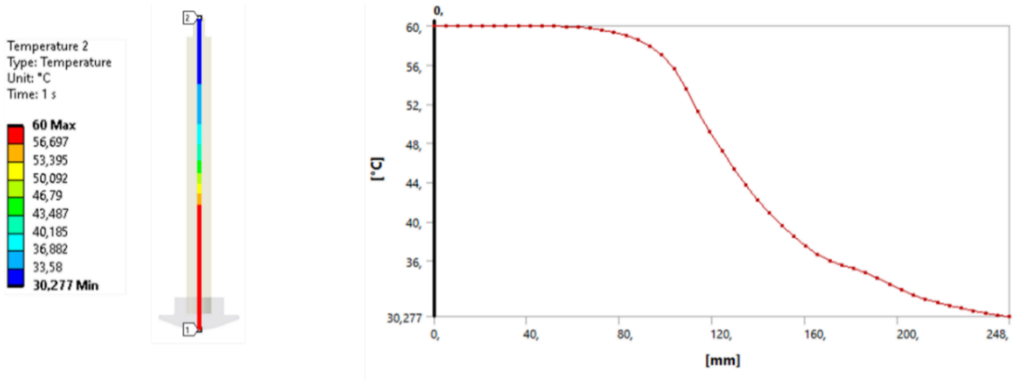


**Figure 20 –** Temperature Variation along the Shutter-Rod

**Source:** Author, 2025

### 5.4 Boundary Conditions

Regarding the structural boundary conditions, the temperature fields obtained from the thermal analysis (Figure 19) and the pressure fields from the flow analysis (CFD) (shown in Figure 21) were imported. These results were applied as loads on the internal surfaces of the valve body.

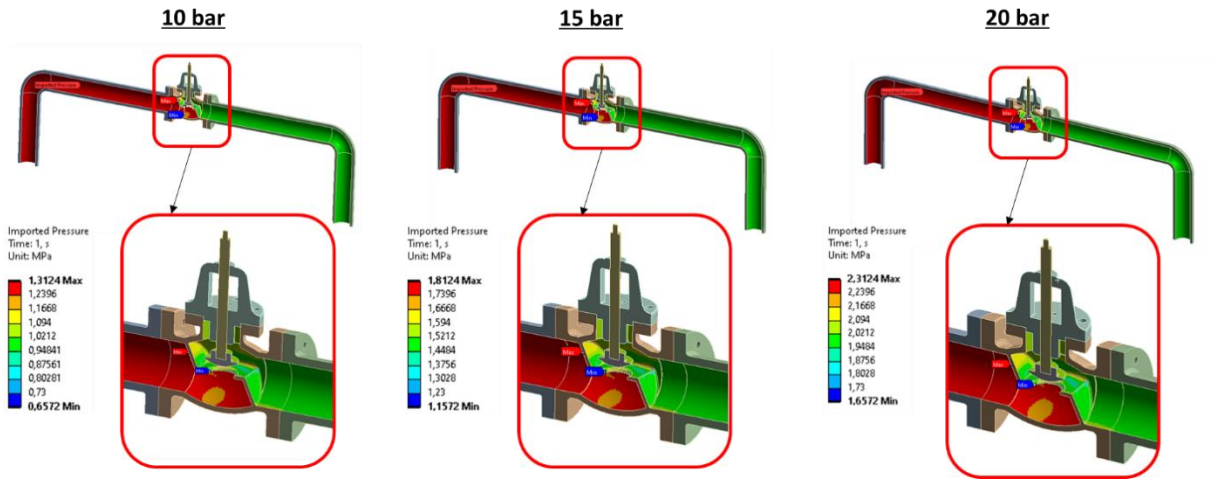


**Figure 21 –** Imported Pressure Fields

**Source:** Author, 2025

Regarding the constraint conditions, the lower surfaces of the tubes were fixed (*Fixed Support), and a Frictionless Support was placed on the surfaces dividing the structure* to represent symmetrical behavior, as shown in Figure 22. Regarding the contacts, all were considered bonded (*Bonded*) except for the contact between the rod and the lower part of the castle where the rod slides with friction. In this case, a frictional contact (*Frictional*) with a friction factor of 0.12 was adopted. Figure 23 illustrates these contacts.

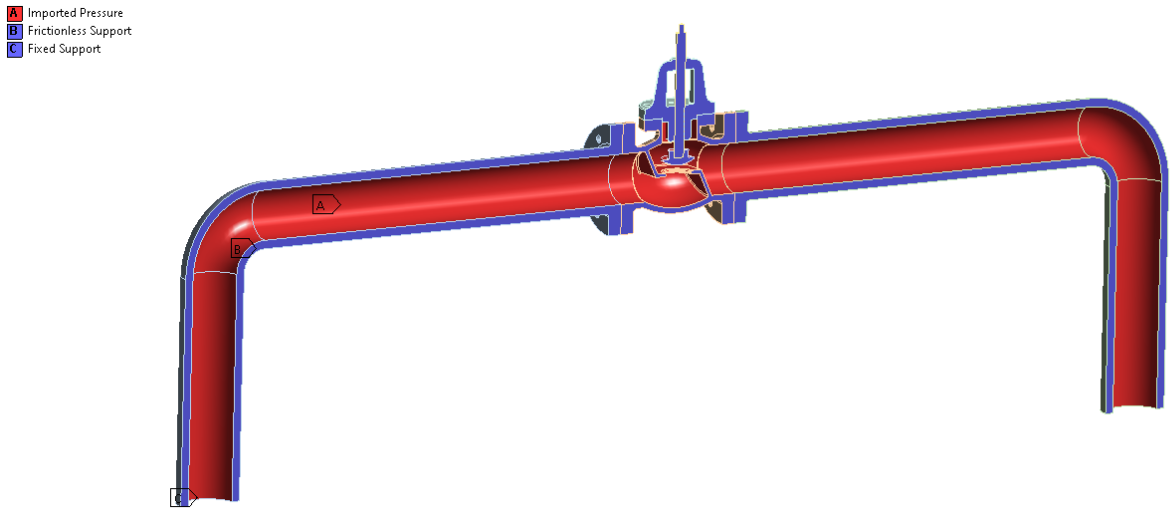


**Figure 22 –** Restriction Conditions

**Source:** Author, 2025

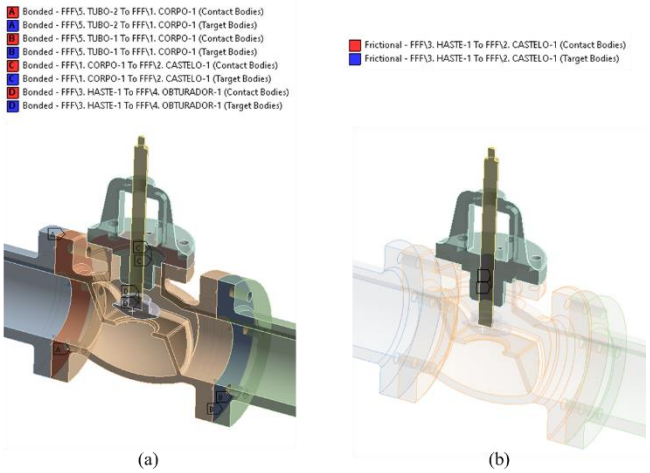


**Figure 23 –** Contact Conditions – (a) *Bonded* and (b) *Frictional*

**Source:** Author, 2025

### 5.5 Structural Mesh

Regarding the structural mesh, a mesh convergence process was performed to ensure that the analysis results did not depend on the size of the elements used. This process consists of progressively refining the mesh and comparing the values obtained for a variable of interest (generally Von Mises stress) until the variation between successive refinements becomes negligible. When this occurs, the mesh is considered to have reached convergence and adequately represents the behavior of the model. Table 2 and Figure 4 show the mesh convergence process for each valve component.

| Body | | |
|---|---|---|
| **Elements** | **Stress** | **Variation** |
| 148276 | 52,32 | - |
| 185804 | 58,90 | 12,56% |
| 250245 | 59,96 | 1,80% |

| Bonnet | | |
|---|---|---|
| **Elements** | **Stress** | **Variation** |
| 90828 | 26,65 | - |
| 112194 | 27,77 | 4,20% |
| 167176 | 28,30 | 1,90% |

| Stem | | |
|---|---|---|
| **Elements** | **Stress** | **Variation** |
| 33957 | 6,46 | - |
| 36760 | 6,90 | 6,72% |
| 40290 | 7,23 | 4,88% |

| Disc | | |
|---|---|---|
| **Elements** | **Stress** | **Variation** |
| 32951 | 0,749 | - |
| 34958 | 0,725 | 3,14% |
| 40093 | 0,727 | 0,23% |

**Table 2 –** Mesh Convergence

**Source:** Author, 2025


**Figure 24 –** Graphs of Mesh Convergence

**Source:** Author, 2025

Since the objective of this work is the structural evaluation of the valve components, greater attention was given to the local refinements and mesh generation criteria of these components. Regarding the pipes, a global refinement was performed to ensure proper coupling between the valve and the piping, guaranteeing the correct transfer of forces. Furthermore, there was sufficient computational capacity to perform the calculation with this level of detail without compromising the simulation performance.

During the creation and convergence of the valve component mesh, regions with higher stress gradients were identified, especially near geometric discontinuities and contact areas between components, as shown in Figure 25. In these regions, a local mesh refinement was applied to increase the accuracy of the results. Figure 26 shows the final mesh used.

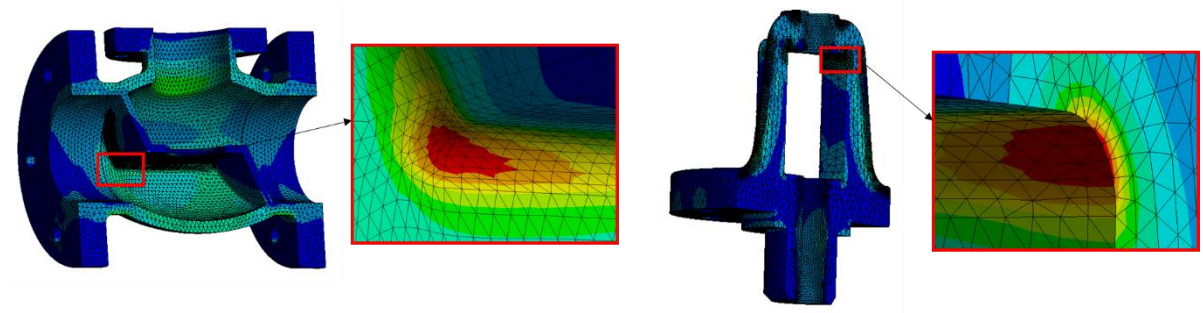

**Figure 25 –** Examples Local Mesh Refinement

**Source:** Author, 2025

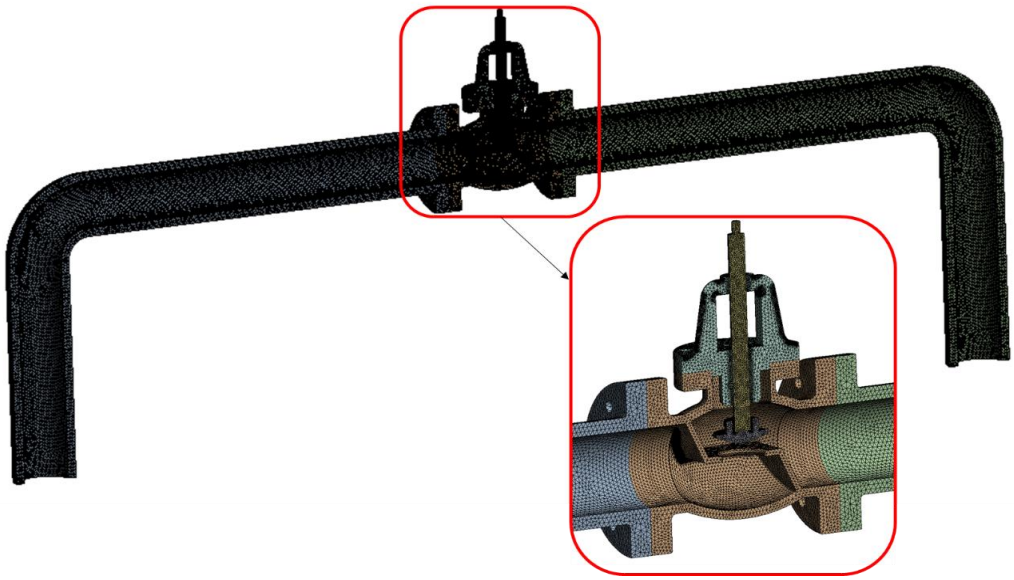

**Figure 26 –** Mesh for Structural Analysis

**Source:** Author, 2025

The quality criteria of the structural mesh were also evaluated, a fundamental step to ensure the accuracy and numerical stability of the results obtained. Assessing mesh quality is important because elements with distorted or disproportionate geometry can generate errors, poor convergence, and non-physical results, especially in regions with high stress gradients.

*Element Quality* stands out , indicating how close the element is to its ideal shape. Values close to 1 represent well-formed elements, while low values indicate undesirable geometric distortions. Another parameter analyzed was the Aspect Ratio , which indicates the relationship between the largest and smallest dimensions of an element. Very high values suggest elongated elements, which can compromise the accuracy of the solution.

Figures 27 and 28 show the distribution of these parameters in the generated mesh. The average value of *Element Quality* was 0.81495 and the *Aspect Ratio* was 1.9633, showing that most elements are within the recommended ranges, ensuring adequate element quality for structural analysis.

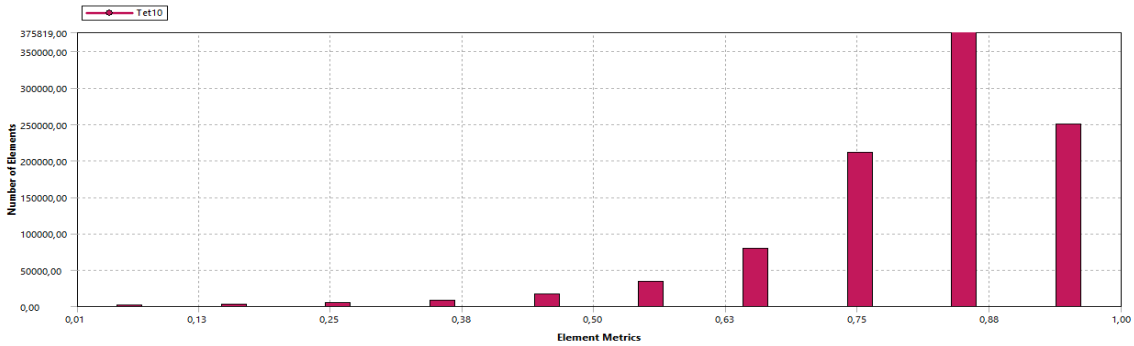


**Figure 27 –** Mesh Quality Criteria - *Element Quality* .

**Source:** Author, 2025

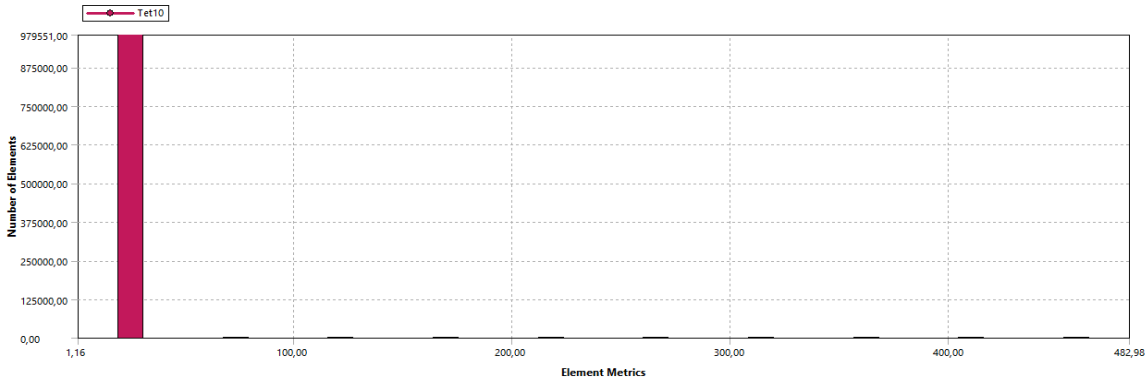


**Figure 28 –** Mesh Quality Criteria – *Aspect Ratio* .

**Source:** Author, 2025

## 5.6 Numerical Convergence

Because this is a problem involving frictional contacts, the nature of the analysis is non-linear. The default ANSYS (*Program Controlled*) settings were maintained for numerical convergence. Figure 29 shows the convergence of the problem.


**Figure 29 –** Numerical Convergence

**Source:** Author, 2025

## 6. STRUCTURAL RESULTS

Figures 30 to 35 present the results for Von-Mises Stress and Displacements under different conditions.

## 6.1 Von-Mises Stress

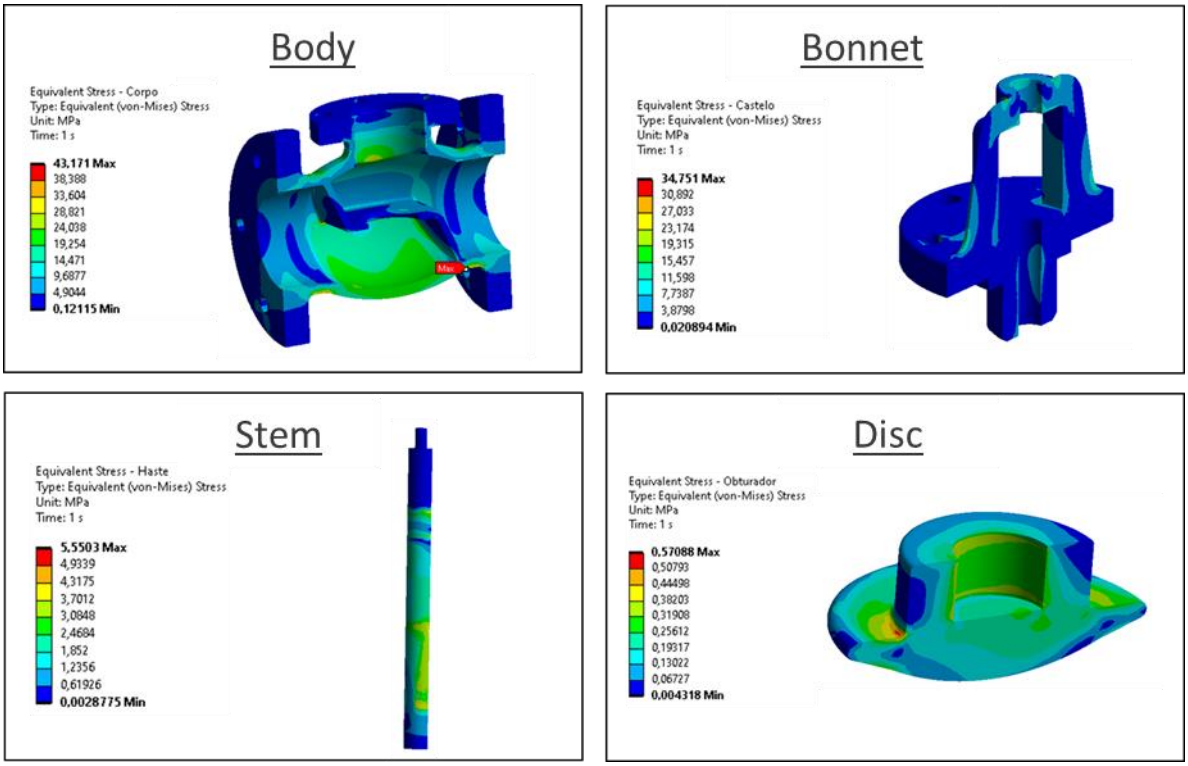


**Figure 30 –** Von-Mises Stress for the Components – Outlet Pressure 10 bar

**Source:** Author, 2025

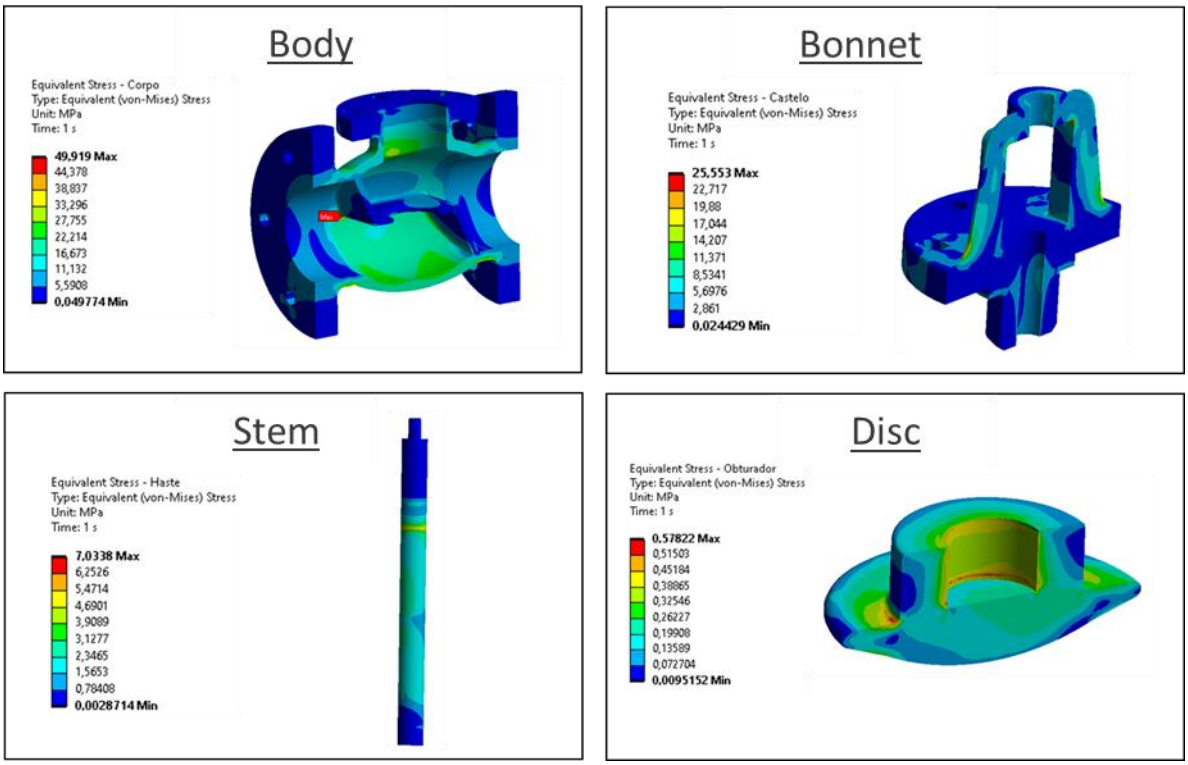


Figure 31 – Von-Mises Stress for the Components – Outlet Pressure 15 bar

Source: Author, 2025

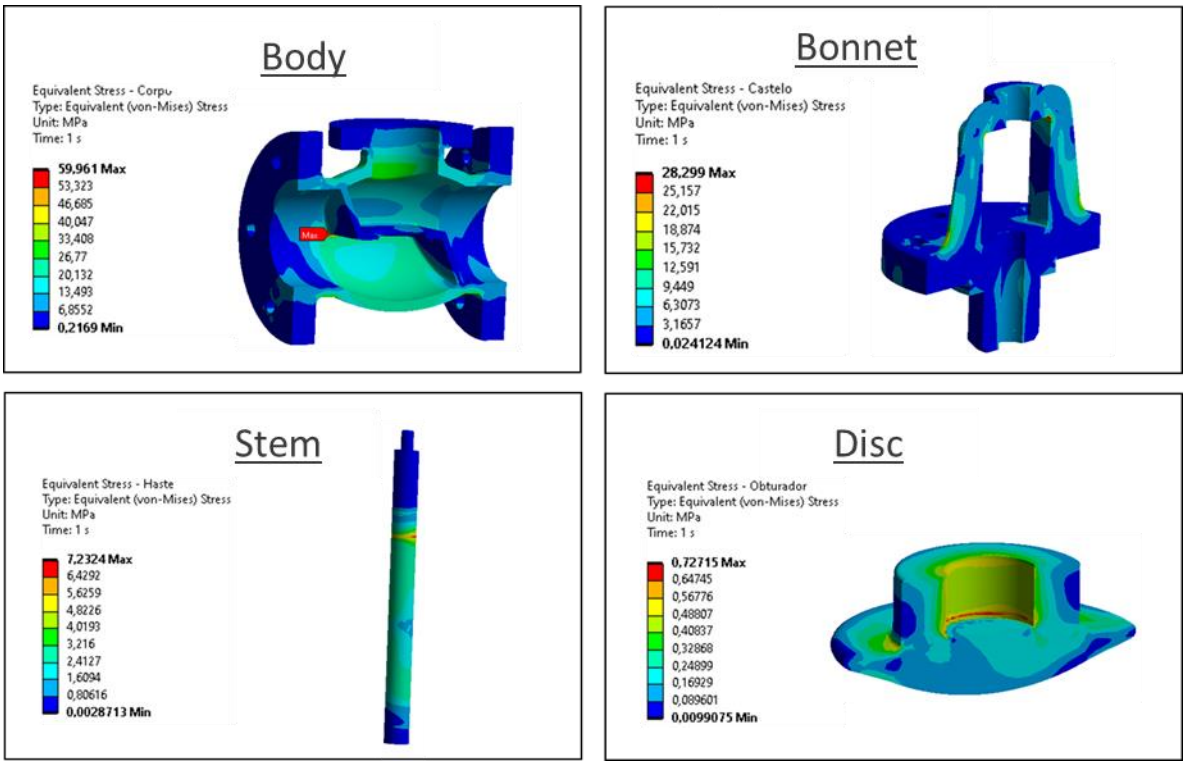


**Figure 32 –** Voltages for the Components – Outlet Pressure 20 bar

**Source:** Author, 2025

## 6.2 Displacements

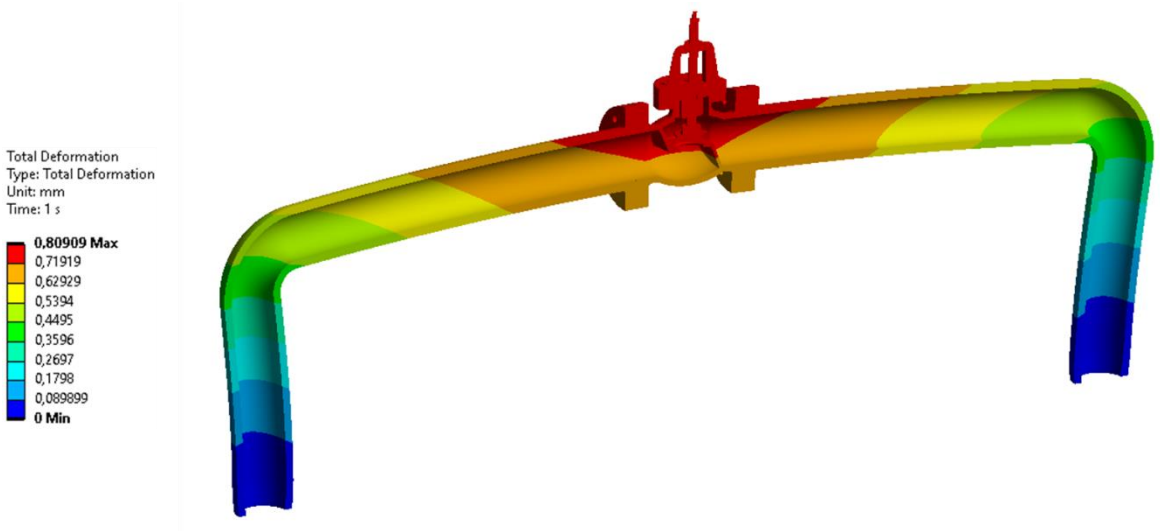


**Figure 33 –** Displacement – Outlet Pressure 10 bar

**Source:** Author, 2025

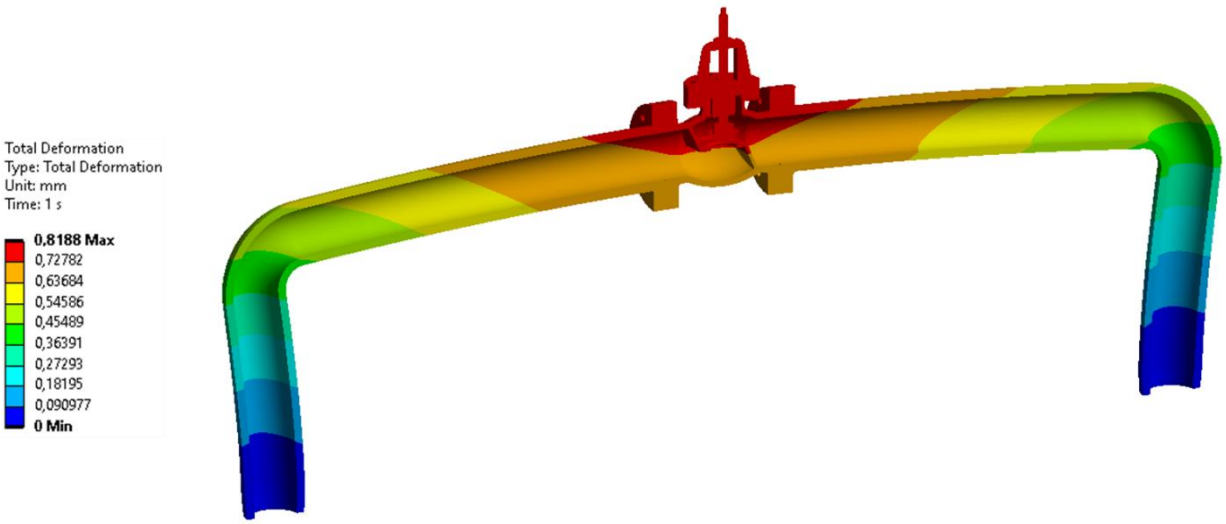


**Figure 34 –** Displacement – Outlet Pressure 15 bar

**Source:** Author, 2025

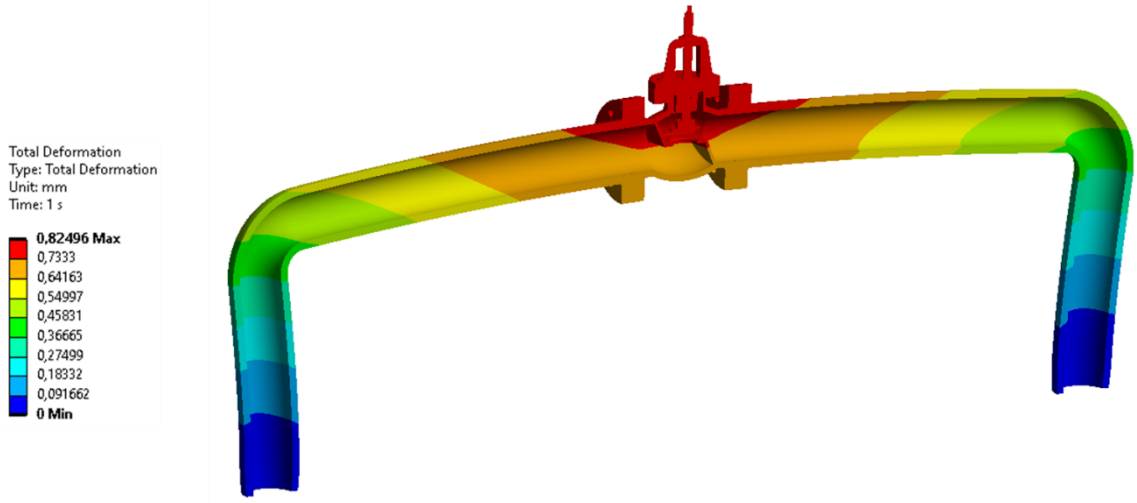


**Figure 35 –** Displacement – Outlet Pressure 20 bar

**Source:** Author, 2025

It was observed that the maximum valve displacement occurs in the central region of the valve. A quantitative comparative analysis of the stresses and displacements obtained will be performed next.

### 6.4 Comparison

A comparison was made of the results for Von-Mises Stress, Safety Factors, and Displacements, as indicated in Tables 3, 4, and 5, respectively.

| | Body | Bonnet | Stem | Disc |
|---|---|---|---|---|
| Pout [Bar] | Von-mises Stress [MPa] | Von-mises Stress [MPa] | Von-mises Stress [MPa] | Von-mises Stress [MPa] |
| 10 | 43,17 | 34,75 | 5,55 | 0,571 |
| 15 | 49,92 | 25,55 | 7,03 | 0,578 |
| 20 | 59,96 | 28,30 | 7,23 | 0,727 |

**Table 3 –** Comparison of Von-Mises Sr

**Source:** Author, 2025

| | Body | Bonnet | Stem | Disc |
|---|---|---|---|---|
| Pout [Bar] | Safety Factor | Safety Factor | Safety Factor | Safety Factor |
| 10 | 5,8 | 7,2 | 49,5 | 482 |
| 15 | 5,0 | 9,8 | 39,1 | 476 |
| 20 | 4,2 | 8,8 | 38,0 | 378 |

**Table 4 –** Safety Factor Comparison

**Source:** Author, 2025

| Pout [Bar] | Max. Displacement [mm] |
|---|---|
| 10 | 0,8091 |
| 15 | 0,8188 |
| 20 | 0,8250 |

**Table 5 –** Comparison of Displacements

**Source:** Author, 2025

As can be observed, the greatest stresses occurred in the valve body, the region that concentrates the main forces resulting from internal pressure and thermal gradients. It was also found that, for some components, the location of the maximum stresses varied according to the applied outlet pressure, indicating an interaction between thermal and pressure effects on the structural behavior.

In the specific case of the valve body, it was observed that the stresses obtained for a pressure of 10 bar were higher than those found for 15 and 20 bar. This behavior is associated with the coupling between thermal stresses and pressure stresses. Under certain conditions, increasing the pressure can counterbalance local thermal effects, resulting in lower equivalent stresses. This phenomenon also explains the changes observed in the region of concentration of

maximum stresses in some components as a function of pressure conditions, since the interaction between the thermal and pressure fields can alter the stress distribution.

This result highlights the importance of considering the combined effect of temperature and pressure in thermo-fluid-structural analyses, since the behavior is non-linear and can vary significantly depending on the operating regime.

Regarding the displacements found, it was observed that they were of low magnitude. Therefore, the use of one-way coupling (FSI) proved to be adequate, since the structural deformations exert a negligible influence on the fluid flow, ensuring good accuracy in the results with lower computational cost.

As can be seen from the safety factors obtained, all valve components showed stresses significantly lower than the yield strength of the material under all operating conditions analyzed. This result indicates that the valve operates in a structurally safe condition, without risk of plastic deformation or overload failure in the situations evaluated.

Based on the results obtained, it is possible to establish a correlation between the maximum stress, which occurs in the valve body, and the operating pressure, as well as between the total displacement and the fluid outlet pressure, as shown in Figure 36. These relationships allow for an integrated evaluation of the valve's structural behavior under different applied load conditions.

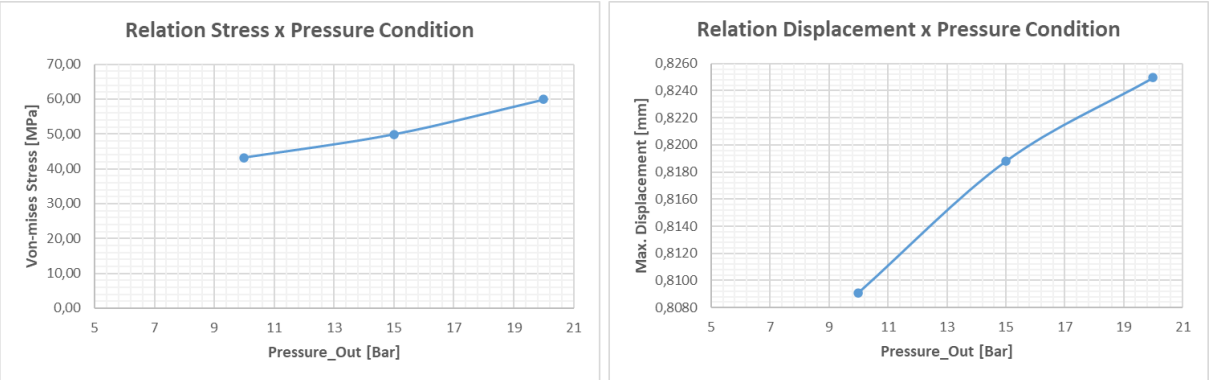


(a) (b)

**Figure 36 –** Relationship between Stress and Pressure Condition (a) and Displacement and Pressure Condition (b)

**Source:** Author, 2025

## 7. CONCLUSIONS

This work made it possible to perform a coupled thermo-fluid-structural (FSI) analysis of a globe valve, allowing for an integrated understanding of the fluid and structural behavior under different operating conditions. Pressure and velocity fields for the fluid under different

flow conditions were obtained through an analysis in Fluent, as well as temperature fields through a steady-state thermal analysis.

Based on the solution of this multiphysics coupling, by importing the obtained pressure and temperature fields, it was possible to identify the stresses and displacements in all valve components, correlating the operating conditions with the observed maximum stress and total displacement. Furthermore, the study highlighted the importance of considering the interactions between thermal and pressure fields, since the combination of these effects can significantly alter the stress distribution and influence the structural behavior of the assembly.

The results demonstrated that, under all conditions analyzed, the valve components exhibited stresses well below the yield strength of the materials, indicating safe structural behavior and validating the efficiency of the numerical model proposed for the study.

## REFERENCES


AMERICAN SOCIETY OF MECHANICAL ENGINEERS. **ASME B16.34 – Valves – Flanged, Threaded, and Welding End** . New York: ASME, 2020.

VERSTEEG, H.K.; MALALASEKERA, W. **An Introduction to Computational Fluid Dynamics: The Finite Volume Method** . 2nd ed. Harlow, England: Pearson Education Limited, 2007.

INCROPERA, F. et al; **Fundamentals of Heat and Mass Transfer** . 7. ed. Hoboken, NJ: John Wiley & Sons, 2011. 1048 p.

THE ENGINEERING TOOLBOX. **Surface emissivity coefficients** . Available at: https://www.engineeringtoolbox.com/emissivity-coefficients-d_447.html .

ESSS Institute. **Lecture Notes** . Specialization in Numerical Analysis Using the Finite Element Method. Florianópolis: ESSS Institute.